Journal of Petroleum Science and Engineering 203 (2021) 108647

Contents lists available at ScienceDirect

Journal of Petroleum Science and Engineering

journal homepage: http://www.elsevier.com/locate/petrol

Microfluidic investigation of enhanced oil recovery: The effect of aqueous floods and network wettability

Marzieh Saadat [a], Junyi Yang [b], Marcin Dudek [a], Gisle Øye [a,*], Peichun Amy Tsai [b,**]

[a] Ugelstad Laboratory, Department of Chemical Engineering, Norwegian University of Science and Technology (NTNU), Norway
[b] Department of Mechanical Engineering, University of Alberta, Canada

ARTICLE INFO

Keywords:
Wettability alteration
Microfluidics
Surfactant flooding
Oil recovery
Enhanced oil recovery
Low salinity water flooding

ABSTRACT

Rock wettability significantly influences underground oil extraction efficiency during enhanced oil recovery (EOR) processes. We experimentally examine the effect of wettability on oil recovery at pore-scale using microfluidics. Glass micromodels are used to mimic the quartz surfaces of hydrophilic porous rocks (such as sandstone), and their wettability is altered chemically with a hydrophobic coating to simulate oil-adsorbed hydrophobic surfaces. Comprehensive and systematic investigations are carried out, considering various crucial factors, namely crude oil components, flood type, as well as brine concentration and composition. A model oil, two crude oils with different chemical compositions, and various aqueous floods containing brine, surfactant, and brine-surfactant solutions are utilized. We record flood patterns and measure the global recovery factor to assess the effect of wettability alteration. Based on the pore-scale observations, water contact angles increase from tests with initially hydrophilic networks to those with hydrophobic ones. Two types of network designs are utilized in this study, a uniform network and a rock network. A layer of oil covers the pore walls and stays intact during the flood in hydrophobic rock networks. Generally, the recovery is lower in rock networks with smaller and dead-end pores. For brine floods, in water-wet networks, the recovery decreases with increasing ionic strength and divalent ions, whereas it is the opposite for the oil-wet ones. In the case of surfactant floods, presence of brine and its ionic strength have different effects on the recovery. One fundamental difference between the brine and surfactant floods proved to be the continuous recovery by the surfactant, i.e., the recovery does not reach a steady state. Finally, surfactant floods as the tertiary method of recovery proved to be more efficient than the brine-only for the experimental conditions explored.

1. Introduction

The extraction of petroleum from a hydrocarbon reservoir is a complex process involving multiple steps due to the interplay between hydrodynamics, wetting, and interfacial interactions. After primary and secondary recovery, where pressure plays the leading role, the tertiary oil recovery often targets modification of forces acting on the oil trapped in small pores. The latter is greatly influenced by surface chemistry, where capillary forces and wettability have a significant contribution at pore-scale. Depending on the nature of the rock formation i.e., rock composition, it can generally be classified as mostly water- or oil-wet (Kamal et al., 2017). However, the entire rock formation is usually not homogenous in structure and surface properties; hence a mixed-wet situation is primarily present. This can be explained by the saturation history of the rock pores. Brine occupied all the pores initially, and the rock was water-wet. Subsequently, crude oil migrated into the rock and altered the wettability towards oil-wet by the adsorption of interfacially active fractions like resins and asphaltenes (Alvarado et al., 2014; Anderson, 1986; Bobek et al., 1958). The crude oil-brine-solid interactions can be in form of surface precipitation or polar, acid/base, and other specific interactions as described by Buckley and Liu (1998). Because of relatively smaller capillary pressure, oil can occupy the bigger pores more easily. Therefore, the smaller pores are left water-wet and overall, the rock is categorized as mixed-wet. This wettability alteration depends on the oil composition, injected fluid, and surface type (Farooq et al., 2011; Nourani et al., 2016; Pradilla et al., 2016;

* Corresponding author. Trondheim, 7491, Norway.
** Corresponding author. Edmonton, T6G 1H9, Canada.
E-mail addresses: Marzieh.saadat@ntnu.no (M. Saadat), jyang2@ualberta.ca (J. Yang), marcin.dudek@ntnu.no (M. Dudek), gisle.oye@chemeng.ntnu.no (G. Øye), peichun.amy.tsai@ualberta.ca (P.A. Tsai).

https://doi.org/10.1016/j.petrol.2021.108647
Received 26 September 2020; Received in revised form 12 February 2021; Accepted 3 March 2021
Available online 11 March 2021

Subramanian et al., 2018).

The natural rock wettability and wettability alterations induced by the oil and water phases can influence the mobilization and displacement of oil, and, therefore, overall recovery. Capillary number (Ca) and viscosity ratio (M) are traditionally utilized to characterize flows during fluid-fluid displacement. The immiscible fluid-fluid displacement can be either stable (with a full displacement and high sweep efficiency) or unstable. The latter is manifested in viscous and capillary fingering. M is commonly defined as the viscosity ratio of the injected phase to the resident fluid. When $M < 1$, the interfacial profiles are unstable with fingering patterns, and higher capillary numbers can lead to less unstable displacements and better recovery factors (Zhang et al., 2011). Generally, capillary number is defined as $Ca = \mu_f V/\gamma$, with the characteristic velocity of the flood (V), viscosity of the flood (μ_f), and interfacial tension between the resident oil and the flood (γ). However, this definition does not reflect the change in wettability. Therefore, some authors have suggested to incorporate contact angle so that $Ca = (\mu_f V)/(\gamma \cos\theta)$, where θ is the contact angle with the surface through the aqueous phase. Capillary pressure is defined as $P_c = P_o - P_w$, where P_o and P_w are the liquid pressure of the oil and water phase, respectively. For positive values of capillary pressure, spontaneous imbibition happens. In contrast, negative capillary pressure in case of imbibition implies that more water pressure is needed to displace more oil. For most of the saturation range, the capillary pressure in water-wet systems is positive. As the wettability changes towards oil-wetness, the capillary pressure can be both positive or negative, meaning that some of the surface imbibes oil and some imbibes water (Abdallah et al., 2007). At lower water saturations, oil relative permeability (k_{ro}) is higher for a hydrophilic system, while at higher water saturations, water relative permeability (k_{rw}) is lower for the hydrophilic system due to the oil occupying the larger pores (Abdallah et al., 2007).

To extract more oil, the capillary forces that help trap the oil in rock pores after waterflooding can be overcome by increasing Ca. One way to approach this would be to decrease the interfacial tension (IFT) using surfactants. Surfactants mobilize residual oil by lowering IFT between oil and water and/or by the wettability alteration from oil-wet to water-wet (Mohammed and Babadagli, 2015; Wang and Mohanty, 2015). The effect of surfactant flooding on oil displacement has been an active topic (He et al., 2014; Hematpour et al., 2012a; Howe et al., 2015; Jamaloei and Kharrat, 2010). Nilsson et al. (2013) provided a reference graph as a guide to design floods with specific viscosity characteristics and showed that surfactant solutions lowered the IFT by a factor of 10 and recovered 15% more oil than water flooding at the same flow rate. He et al., 2014, 2015 utilized two types of weakly emulsifying and non-emulsifying surfactants to recover oil from an oil-wet micromodel of random porous network. By comparing the oil recovery efficiencies using the two stimulation fluids, they concluded that the former type is more efficient. In the study by Howe et al. (2015), commercial anionic surfactants were used, and different types of microemulsions (oil-in-water, water-in-oil, and bi-continuous) were produced. The study showed that microemulsion formation was the primary mechanism of oil recovery, where the bi-continuous type showed to be the most effective in sweep efficiency with a sharp and well-defined liquid front. Water-in-oil microemulsion left more residual oil behind the rough front, and oil-in-water microemulsion resulted in only moderate recovery because of low water-oil interfacial tension. Surfactant flooding has been tested in several oil fields around the world (Kamal et al., 2017). Anionic surfactants are the most common surfactants in chemical enhanced oil recovery (EOR) applications in sandstone, out of which compounds with sulfonate groups are the most widely used (Bera and Mandal, 2015; Kamal et al., 2017). Surfactants, sodium dodecylbenzenesulfonate (SDBS) and sodium dioctyl sulfosuccinate (AOT) were used by Nourani et al. (2014), Tichelkamp et al. (2016), and Jakobsen et al. (2018) for EOR applications and showed promising potential.

Low salinity water flooding as a tertiary oil recovery method has gained a lot of interest in research studies and field tests (Lager et al., 2008a, 2008b; Ligthelm et al., 2009; McGuire et al., 2005; Seccombe et al., 2008; Tang and Morrow, 1997). The method is more cost effective and environmentally friendly than other chemical EOR methods. The method efficiency also depends on the brine salinity and composition (Morrow and Buckley, 2011; Yousef et al., 2012). Although there have been many studies on the subject, a consistent mechanism is not yet agreed upon (Katende and Sagala, 2019; Morrow and Buckley, 2011). The suggested mechanisms include local increase in pH at the clay surface (Austad et al., 2010; RezaeiDoust et al., 2011), fine migration (Song and Kovscek, 2016; Yu et al., 2019), multicomponent ionic exchange (Lager et al., 2008a), destabilization of oil layer (Alagic et al., 2011; Spildo et al., 2012), and wettability alteration (Ding and Rahman, 2017; Mahani et al., 2013; Mohammed and Babadagli, 2015; Sharma and Mohanty, 2018) among others.

Flooding with both surfactant and brine solutions typically surpasses the effect of either flood alone (Alagic and Skauge, 2010). The synergy combines both low salinity and surfactant recovery mechanisms as the low salinity brine helps *via* the mechanisms mentioned above, and the surfactant solution reduces the IFT and modifies the surface wettability. Consequently, low salinity surfactant flooding facilitates recovering additional oil and improves the water wettability of the reservoir. The low salinity brine also helps with decreasing surfactant precipitation and retention, which are challenges associated with surfactant flooding (Alagic and Skauge, 2010). At higher capillary forces, oil gets re-trapped easily. Therefore, with decreasing these forces/increasing capillary number by adding surfactants, re-trapping of the destabilized oil is avoided (Alagic and Skauge, 2010; Alagic et al., 2011; Glover et al., 1979; Johannessen and Spildo, 2013; Spildo et al., 2012, 2014). Moreover, the use of surfactants at low salinity provides the opportunity to achieve low-cost surfactant systems, while also offering an increased chance of meeting safety and environmental regulations (Alagic and Skauge, 2010).

Most experimental studies concerning the recovery of oil have been done using core flooding. Due to the advent of microfabrication, microfluidics has become increasingly popular for probing different parameters affecting oil recovery by providing clear pore-scale observations (Buchgraber et al., 2012; He et al., 2015; Howe et al., 2015; Lifton, 2016; Song and Kovscek, 2015). Moreover, the microfluidic method is less time-consuming. Wettability is a major parameter that can affect capillary pressures, relative permeabilities, fingering mechanisms, and saturations in multiphase flow in porous media (Anderson, 1987). Some researchers have tried altering the wettability of the network (Buchgraber et al., 2012; Schneider and Tabeling, 2011; Song and Kovscek, 2015; Wegner et al., 2015). Song and Kovscek (2015) modified the wettability properties through the irreversible adsorption of clay particles on silicon surfaces. In another study (Schneider and Tabeling, 2011), the wettability of the PDMS micromodels was selectively altered in uniform and non-uniform patterns by UV-initiated graft polymerization. Coating with alkyl silanes is also a common method used in the literature and industry to modify surfaces, including silicates (Arkles, 1977; Eckstein, 1988; Grate et al., 2013; Naik et al., 2013). Surface wettability plays a vital role in oil recovery. Particularly, it is important to understand how different brines or surfactants can affect the rock wettability and subsequent oil recovery. Performing tests on both initially water-wet and initially oil-wet structures is therefore needed to contribute to a better understanding of the oil-brine-rock interplay, particularly addressing the influence of oil and water phase components on the recovery.

The objective of this study is to investigate the effect of rock wettability on the recovery process and the recovery factor through microfluidics. The microfluidic methodology enables us with visual observation of the recovery process, and how the wettability and contact angle change with different parameters, which would have been challenging with the classical method of studying EOR, core flooding. Using both rock-like and uniform microfluidic networks, surfactant and brine floods, different compositions of floods, and different crude oils, we

Table 1
Physicochemical properties and compositions of crude oils (Dudek et al., 2018).

	API [°]	Viscosity [mPa.s] @20 °C	TAN [mg KOH/g oil]	TBN [mg KOH/g oil]	SARA [% wt.]			
					Saturates	Aromatics	Resins	Asphaltenes
Crude oil A	19.2	354.4	2.2	2.8	50.6	31.2	15.7	2.5
Crude oil C	23	74.4	2.7	1.1	64.9	26.3	8.4	0.4

Table 2
Displacing fluid properties.

Flood	Symbol	NaCl concentration (M)	Ca/Na (mole/mole)	Surfactant concentration (mM)	IFT with crude oil A (mN/m)	IFT with crude oil C (mN/m)
High salinity brine	HS-Na	0.6	0	0	13.05	15.52
High salinity brine	HS-NaCa	0.566	1/50	0	13.26	15.1
Low salinity brine	LS-Na	0.02	0	0	19.40	18.60
AOT + high salinity brine	HS-AOT	0.3	0	2.47	0.262	–
AOT + low salinity brine	LS-AOT	0.02	0	2.47	0.345	0.210
AOT (in DI water)	AOT	0	0	2.47	2.83	3.28
SDBS + high salinity brine	HS-SDBS	0.3	0	1.25	0.183	–
SDBS + low salinity brine	LS-SDBS	0.02	0	1.25	1.345	0.9
SDBS (in DI water)	SDBS	0	0	1.25	6.54	4.85

investigate the effect of wettability on oil recovery.

2. Materials and methods

2.1. Fluids

Xylene was used as a single-component model oil in the initial experiments. A solution of 0.1 wt% Span 80 in xylene was also made to study the effect of the oil-soluble additive on the recovery. Span 80 was added to xylene as the interfacially active component and is a non-ionic oil-soluble surfactant that can form water-in-oil emulsions. Sudan III was used as the dye (at 0.4 wt%) to enhance the contrast between water and oil phases in the micromodel.

Two crude oils from the Norwegian Continental Shelf were used. These crude oils are different in chemical composition, particularly resin and asphaltene contents. This provides a variety of capillary numbers, viscosity ratios, and wetting conditions induced by the oil phase. Table 1 lists the main properties of the two crude oils.

Brines (of high and low salinity) and different brine-surfactant solutions were prepared as the displacing fluids in the experiments. Brines were made either with only monovalent cations (sodium chloride) or both monovalent and divalent cations (sodium chloride and calcium chloride) in de-ionized (DI) water. The divalent to monovalent ion ratio was decided based on typical seawater composition and other studies (Tichelkamp et al., 2015). Surfactant solutions were prepared in DI water, high salinity brine (HS-surfactant), and low salinity brine (LS-surfactant). Two anionic surfactants, sodium dodecylbenzenesulfonate (SDBS) and sodium dioctyl sulfosuccinate (AOT) were used in this study. SDBS is a common sulfonate surfactant with a single hydrophobic tail, while AOT is a double-tailed surfactant, typically used in reverse micelle systems (Flynn and Wand, 2001; Kamal et al., 2017). Surfactant concentrations were set lower than critical micelle concentration (CMC) and were decided based on different values reported in the literature (Dubey, 2009; Forland et al., 1998; Hait et al., 2003; Tichelkamp et al., 2014, 2015). Table 2 presents the properties of the displacing floods.

The density and viscosity of the fluids were measured with a density meter (DMA-5000 M, Anton Paar) and a rheometer (Physica MCR 301, Anton Paar), respectively. The interfacial tension between different oil and water phases were also measured with a spinning drop tensiometer (SVT 20 N, DataPhysics Instruments).

2.2. Experimental setup and porous media

The experimental setup includes a flow setup, an imaging setup, a pressure sensor, and a microfluidic device as described in our previous study (Saadat et al., 2020). The syringe pump (Chemyx Fusion 4000) is used for flooding the chips during the experiments, and injecting solvents during the cleaning procedure. The micromodel is connected to inlet and outlet tubing for fluid injection and extraction through a chip holder. A high-resolution camera (Canon EOS 90D) fitted with a macro lens was used to capture the images using the computer software. The pressure sensors by Labsmith and ElveFlow were used to record the pressure during flooding. Some images from selected tests are also acquired utilizing a microscope (Nikon ECLIPSE Ti2–U) and an attached camera (Photron FASTCAM Mini WX100) for a microscopic view of the oil and water phase arrangement within the channels.

Two different designs of micromodels from Micronit Microtechnologies are used. One is a model system of interconnected channels of 50 μm wide and 20 μm deep denoted as uniform network with an internal volume of 2.1 μl. The other is a replica of a cross section of a carbonate rock as a better representation of reservoir rock called rock network with an internal volume of 2.3 μl. Both types are made from borosilicate and are naturally hydrophilic. The porosity of the uniform and rock network are 0.52 and 0.57, respectively. All tests are performed with uniform network chips unless stated otherwise.

2.3. Hydrophobization

To assess the effect of wettability, we altered the hydrophilic nature of the glass micromodels towards oil-wetness with a 0.2 wt% solution of octadecyl trichlorosilane (OTS) in toluene. The OTS solution was injected into the micromodel and left for 15 min before it was withdrawn again. Before the chips could be used, they were left to dry for 24 h at ambient conditions to ensure the evaporation of all remaining solvent. Contact angles of DI water on the original and treated flat borosilicate wafers (made from the same material as the chips) were measured to test the method's effectivity. The contact angles for the original hydrophilic and modified hydrophobic surfaces were 37.0° and 102.4°, respectively. Due to the OTS treatment, a self-assembled monolayer forms on the glass and results in reduction of surface charges because of the presence of the neutral methyl head groups (Jing and Bhushan, 2013; Lutzenkirchen and Richter, 2013; Stein et al., 2004). Please note that the terms water-wet/hydrophilic and oil-wet/hydrophobic refer to the initial state of the glass chip prior to oil

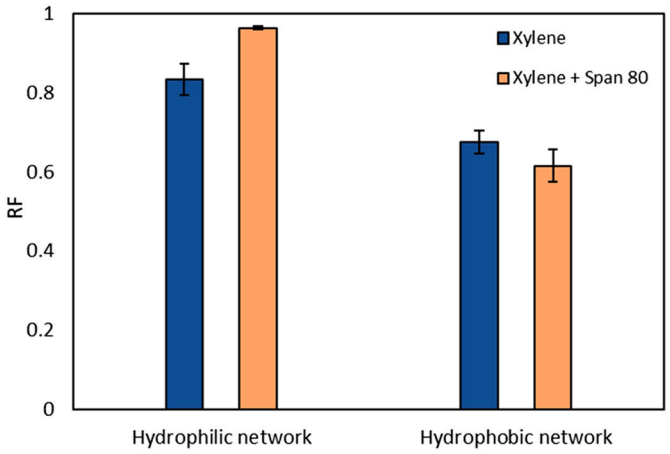

Fig. 1. The effect of adding oil surfactant (Span 80) to xylene on oil recovery by HS-Na in hydrophilic and hydrophobic uniform networks.

saturation, and not the state it might be modified to throughout the test.

2.4. Experimental procedure

The procedure is also derived from a previous study (Saadat et al., 2020). Briefly, for one step recovery tests, the oil phase is injected into the micromodel until the chip is completely filled. 10 μl (4.8 P V for uniform network) of the displacing fluid is subsequently pumped at 0.5 μl/min into the chip. The camera records the displacement process, and the pressure at the inlet is measured.

For EOR tests, the chip is initially filled with high salinity brine (HS–Na) and aged for 30 min to simulate the formation water. The crude oil is then injected into the chip, and the chip is aged in a custom-made aging holder for another 2 h at room temperature. The aging holder was designed to block the inlet and outlet opening of the chip and prevent loss of crude oil during aging of the oil in the chip. Next, 10 μl of high salinity brine (HS–Na) is flooded as the secondary recovery or improved oil recovery (IOR). Finally, the EOR flood (10 μl) is used as the tertiary stage. Every oil recovery experiment is repeated three times to check and ensure repeatability.

The recorded images are processed and analyzed using ImageJ. The process includes color thresholding based on saturation and brightness, and conversion to 8-bit black and white images. Based on the black and white pictures, the oil saturation can be calculated in pixels. Recovery factor (RF) is then calculated as the ratio of recovered oil to the original oil in place. The ImageJ angle tool is used for contact angle measurement. By drawing one line coincident with the pore surface and the other line tangent to the oil meniscus, the contact angle can be measured.

The chips go through a cleaning procedure after each experiment is done. The chips are rinsed with a mixture of xylene and isopropanol (50%/50%), following by de-ionized water. After flushing the chips with air, they are heated up to 475 °C in an ashing furnace to disintegrate and evaporate any possible residues.

3. Results and discussion

3.1. Model oil

To evaluate the effect of interfacially-active components in the oil phase in a controlled way, displacement studies were carried out for xylene and Span 80-xylene. The experiments were conducted in both water-wet and oil-wet networks (Fig. 1).

For both xylene and xylene-surfactant solutions, the RF decreases from the hydrophilic to hydrophobic network by 16% and 35%, respectively. Naturally, there is a higher affinity between the oil and the hydrophobic surface, which justifies the difference in recovery for the two surface types. Consistently, the oil recovery has been reported to be lower from carbonate reservoirs in general, as the more oil-wet type of rocks (Mohammed and Babadagli, 2015; Morrow, 1990; Wagner and Leach, 1959). Comparing the xylene test in water- and oil-wet networks, the breakthrough happens sooner and at a lower flood pore volume in the latter case by 34 s and 0.133 P V on average, respectively. These numbers are even lower for xylene-surfactant in the oil-wet system. The decrease in RF between the hydrophilic and hydrophobic networks, however, is bigger in the case of the xylene-Span 80 solution. This can be explained by the better adsorption of the active component onto the more oil-wet surfaces, as also suggested by previous studies (Kelesoglu et al., 2012; Nourani et al., 2016).

Visual observations from this set of tests reveal stable displacement of the xylene-Span 80, and almost stable displacement for xylene in the water-wet networks, In contrast, the displacements are unstable in the oil-wet networks. The viscosity ratios are 1.8 and 1.7 for xylene and xylene-Span 80 tests, respectively. The similar values of the viscosity ratios also confirm the effect of wettability on the displacement pattern. The images also reveal a rather visible difference between the two wettabilities. More extensive spreading of the oil phase on the channel walls is observed in hydrophobic networks, while the trapped oil in the hydrophilic ones after flooding forms droplets in both xylene and xylene-Span 80 cases (Figure S1).

The results also show that the addition of surfactant to xylene can have different effects depending on the network wettability. For example, Span 80 causes an increased recovery in the hydrophilic network, whereas the same combination shows a lower recovery in the hydrophobic one. The additive decreases the oil-brine IFT substantially.

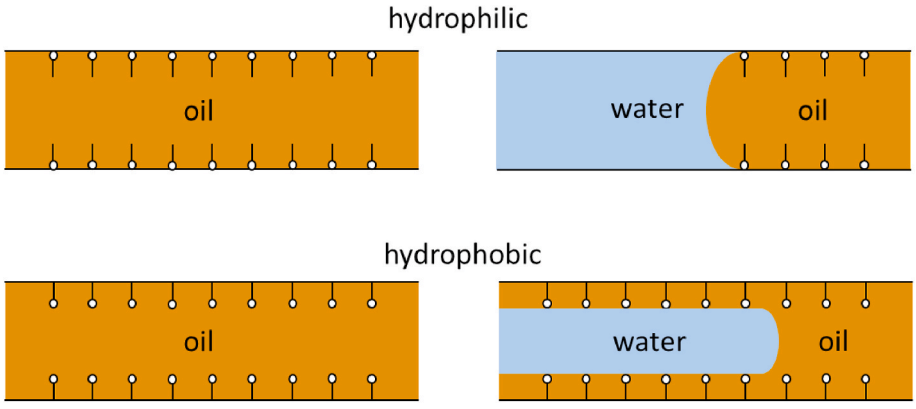

Fig. 2. A simplified molecular demonstration of the water phase displacing the oil phase containing surfactants (schematically shown with a hydrophilic head and a hydrophobic tail) in hydrophilic and hydrophobic channels.

Table 3
Recovery factors for crude oils A and C displaced by HS-Na in hydrophilic and hydrophobic uniform networks.

Wettability	Crude oil A	Crude oil C
Hydrophilic	0.68 ± 0.01	0.72 ± 0.02
Hydrophobic	0.68 ± 0.02	0.89 ± 0.01

The IFT between HS-Na and xylene with and without Span 80 is 2.5 and 38.2 mN/m, respectively. Therefore, there is a negative correlation between RF and IFT for water-wet networks and a positive relationship between the two for oil-wet networks. Based on the negative correlation of IFT and capillary number value, the opposite applies to the wettability-capillary number relationship. Our result is in line with the data from oil-wet rocks, where studies have reported decreasing oil recovery from carbonate rocks with the increase of surface-active components (Austad and Standnes, 2003; Fathi et al., 2011; Ju et al., 2006; Zhang and Austad, 2005). Fig. 2 could demonstrate the displacement process at a molecular level for the system containing surfactants.

3.2. Crude oil

In this section, crude oil is used as the oil phase. Different parameters affecting the recovery, including oil type, water phase, and network design are investigated in both water-wet and oil-wet micromodels.

3.2.1. Oil type

Crude oils can have different defining characteristics that can affect their recovery. In this study, crude oils A and C were tested. The tests include flooding the oil-filled chips with HS-Na in both water- and oil-wet networks. Table 3 lists the RF results for the crude oils displaced by HS-Na in both hydrophilic and hydrophobic uniform micromodels.

Assessing the effect of rock wettability, there is an increase from water-to oil-wet recoveries. Although it is less than 1% for crude oil A, crude oil C shows a more substantial increase of almost 17% in favor of the oil-wet model. Even though studies in the past have suggested lower recovery for carbonate reservoirs, it must be considered that although the wettability of carbonate and OTS-treated surfaces are similar, their surface charges are not. The difference may be explained based on the differences between surfaces. Nourani et al. (2016) stated that acid-base interactions between basic crude oil components (dominant in crude oil A) and weakly acidic silanol groups at the hydrophilic silica surface can happen. However, silanol groups are not exposed at the surface in the case of OTS covered surfaces, it is rather alkyl groups that are present. Pradilla et al. (2016) also showed the importance of polar interactions by showing no adsorption at silica surface for a model compound with aliphatic end groups and no acidic functionality.

Crude oil C also reveals a higher RF than crude oil A in both micromodel wettabilities, showing a more significant recovery gap in the hydrophobic system (20%). The wettability of the reservoir can, to a large degree, be affected by the crude oil compounds adsorbed onto the rock surface (Alvarado et al., 2014; Bobek et al., 1958; Kowalewski et al., 2002; Ogunberu and Ayub, 2005). Crude oil A is more viscous and has a more significant fraction of surface-active components such as asphaltenes and resins that can adsorb on the glass surface and make it less water-wet. However, since the recovery is not affected by the surface wettability, it seems like viscosity is the dominating factor. Crude oil C, on the contrary, has a lower viscosity that leads to a higher recovery.

All these tests went through unstable displacements, with more severe effects for crude oil A, especially in hydrophobic networks. While for hydrophilic networks, the recovery reaches a plateau shortly after the breakthrough with close to zero or small additional oil recovery (Saadat et al., 2020), a substantial amount of additional crude oil A was recovered in the oil-wet network. Even though the RF almost does not change between the two wettabilities for crude oil A, the flood patterns, contact angles, and arrangement of the two phases in the channels certainly vary, as illustrated by the after-flood snapshots (Fig. 3). The top images show the time-lapse of the flooding process from darker to lighter colors. The white color represents the changes after the

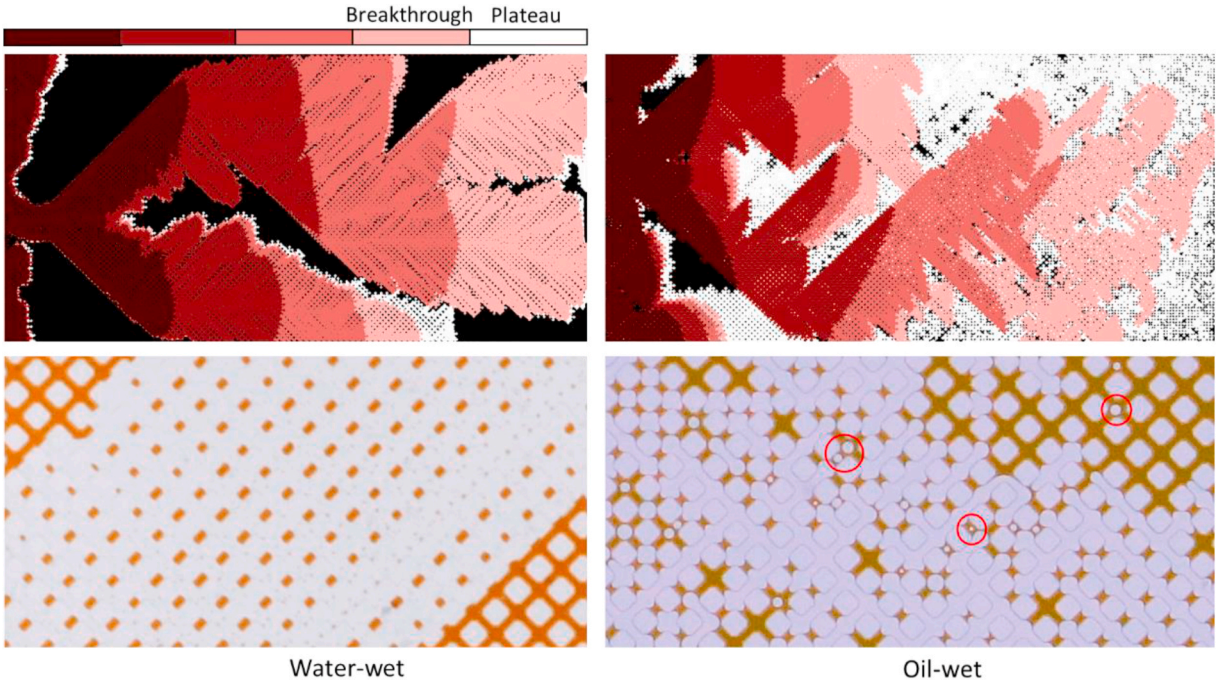

Fig. 3. After-flood images of crude oil A displaced by HS-Na in water-wet and oil-wet uniform network. The top images show the progress of the flood in the whole network area of the micromodels and the bottom row shows close-ups of the channels of the respective network areas, highlighting the arrangement of the two oil and water phases. The breakthrough flood pore volume (PV) for the two are 0.67 and 1.05, respectively. The early stage is represented by the darkest color and the breakthrough by lightest pink. The white area shows the amount of oil recovered after the breakthrough. The voids of the chip (grains) are colored with the same color as the surrounding channels. (For interpretation of the references to color in this figure legend, the reader is referred to the Web version of this article.)

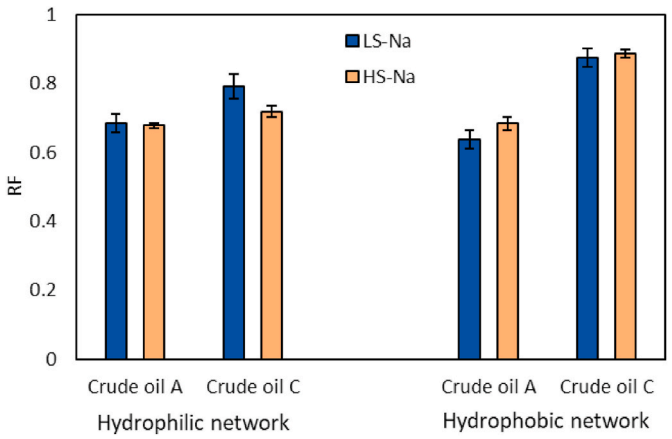

Fig. 4. The effect of brine concentration on RF for crude oils A and C in hydrophobic and hydrophilic systems. Crude oil were displaced by 4.8 P V of brines.

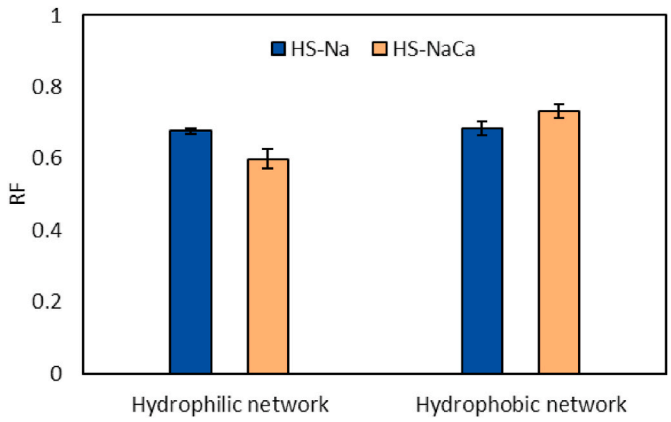

Fig. 5. The effect of divalent ions in the water phase on the RF. The experiment here is crude oil A displaced by high salinity brine in uniform hydrophilic and hydrophobic networks.

breakthrough. The voids of the chip (grains) are colored with the same color as the surrounding channels. The black represents residual oil. The figure also shows the arrangement of the two phases after the flooding in the bottom row pictures, confirming the wettability difference in the networks. The oil has spread visibly on the hydrophobic surface, and water has formed droplets inside the oil phase, as marked. For crude oil C, although the same change in contact angles applies, the displacement pattern does not change as drastically as with crude oil A.

The direct relationship between Ca and RF in the hydrophobic network does not apply in this case as the capillary number for the case of crude oils A and C is 7.0E-6 and 5.9E-6, respectively. Viscosity ratios for the same two cases are 0.004 and 0.019, respectively. Therefore, we see a less unstable movement for crude oil C, where the difference in the viscosity of displaced and displacing fluids is lower.

3.2.2. *Water phase*

Many parameters related to the water phase affect the oil recovery. In this section, water phase parameters are studied across water- and oil-wet models.

3.2.2.1. Salt concentration. The effect of brine concentration in the flood was evaluated on the recovery in systems with different wettabilities. Chips saturated with crude oils A and C were flooded with both high and low salinity brines, HS-Na and LS-Na (Fig. 4).

In the hydrophilic micromodels, the recovery by low salinity brine is higher than high salinity brine, even though it is marginal for crude oil A. This trend is opposite for the hydrophobic networks, i.e., the recovery is slightly lower with low salinity flooding in an oil-wet system. Previous works (Alagic and Skauge, 2010; Alshakhs and Kovscek, 2016; Chavez-Miyauchi et al., 2016; Sheng, 2014; Song and Kovscek, 2015) suggested increased recovery when using low salinity water instead of high salinity in systems with different wettabilities. However, the systems used in this study are different from the natural settings in a few ways including lack of clay particles and multivalent ions, which are said to be major factors in the low salinity water flooding mechanisms (Lager et al., 2008a; Song and Kovscek, 2016; Yu et al., 2019). This could justify the small decrease in recovery for the hydrophobic chips here.

Crude oil C has a higher recovery compared to crude oil A when displaced with LS-Na. As also mentioned in the oil type section, the higher asphaltene and resin fraction of crude oil A could lead to stronger adsorption to the solid surface. This applies to both hydrophilic and hydrophobic network. As a number comparison with core flooding, Alagic et al. (2011) reported a recovery of approximately 45–55% from Berea sandstone cores for a crude oil with similar total acid and base number as crude oil A, but a lower viscosity by low salinity brine as the secondary recovery. In comparison, the recovery we get from a similar secondary recovery microfluidic test is at least 13% higher than the reported number for core flooding.

The capillary numbers for the combinations crude oil A – HS-NA and crude oil A – LS-Na are 7.0E-6 and 4.5E-6, respectively. These numbers for crude oil C are 5.9E-6 and 4.2E-6, respectively. Same as the previous section, there is a negative relationship between the RF and capillary number. The LS-Na flood patterns and their differences in the two micromodels for crude oil A are comparable to those of HS-Na (Fig. 3), albeit with more unstable displacements for crude oil A, especially in hydrophobic networks. However, the changes are not as drastic for crude oil C in terms of differences in flow patterns. The viscosity ratios for crude oil A – LS-Na and crude oil C – LS-Na are 0.004 and 0.018, respectively, which also explains the differences in degrees of instability in oil displacements. Regarding the arrangement of the remaining oil and the brines after the flood, the contact angles slightly increase from high to low salinity brine, specifically visible in the case of crude oil C in the hydrophilic network, and more dramatically from hydrophilic to hydrophobic network (Figure S2). For each pair of tests with low and high salinity flood in hydrophilic networks, the one with the higher RF also has a higher breakthrough time and injected pore volume value. The trend is the opposite in the hydrophobic tests.

3.2.2.2. Presence of divalent ions. To investigate the effect of divalent ions in the water phase, crude oil A was displaced with high salinity brines with and without calcium ions, in both oil- and water-wet chips. For consistency, the ionic strength of the two displacing fluids was kept the same at 0.6 M.

Based on Fig. 5, there is a positive effect on the recovery by having divalent ions in the oil-wet system. In a hydrophilic system, calcium ions can function as a bridge between negatively charged oil components and the surface (Nourani et al., 2016). Therefore, the presence of calcium ions provides a stronger oil adsorption that resists recovery. Better oil adsorption, bound by calcium cations, can shift the surface wettability, the extent of which depends on the ratio of calcium to sodium ions (Khanamiri et al., 2016). However, without many negative sites on the oil-wet surface, the bridging does not happen as extensively. Therefore, a higher RF is observed in the oil-wet system.

In terms of overall displacement patterns, they are similar to the other brine patterns for oil- and water-wet chips. The viscosity ratio for both crude oil A – HS-Na and HS-NaCa is 0.004, which would predict a similar unstable displacement. The degree of branching and spreading, however, is higher in the hydrophobic micromodel. Considering that oil – HS-Na has a slightly higher capillary number than oil – HS-NaCa, a direct relationship between RF and capillary number applies in the water-wet network.

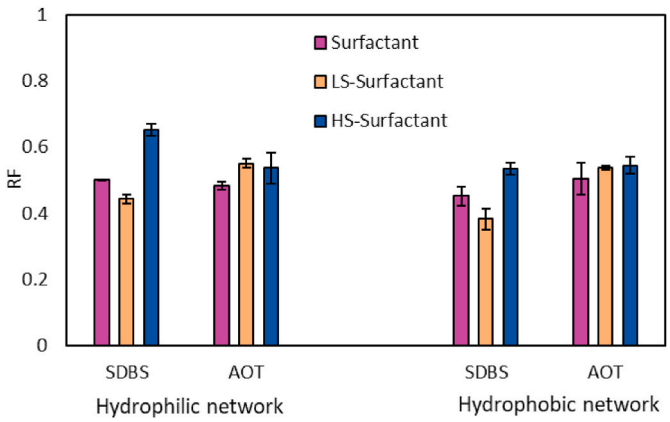

Fig. 6. Recovery of crude oil A by surfactant and brine solutions in uniform water- and oil-wet systems.

3.2.2.3. Surfactant flooding. One way to decrease the IFT and mobilize trapped oil is to use surfactants in the displacing fluid. In this section two types of surfactant, SDBS and AOT, are used to displace crude oil A. Simulated EOR fluids can also include combined surfactant and brine flooding, where the composition (i.e., the type of surfactant and ionic strength) of the aqueous phase can be systematically varied. The combination (of surfactant and brine) is supposed to increase the recovery factor while also improving surfactant loss. Here, solutions of surfactant in DI water, low salinity brine, and high salinity brine are investigated. Fig. 6 demonstrates the RF for the various surfactant solutions, in both hydrophilic and hydrophobic networks.

Comparing each test between the oil- and water-wet networks, SDBS solutions result in higher RFs in hydrophilic networks. The recoveries are higher by 4.8%, 6.1%, and 11.9% than the hydrophobic networks on average for SDBS, LS-SDBS, and HS-SDBS, respectively. However, the wettability of the micromodel does not seem to affect the AOT-flooded tests as much. Anionic surfactants can adsorb on the surface and shift the wettability towards water-wetness in carbonate rocks (Hajibagheri et al., 2017). However, in case of OTS treated surfaces, alkyl chains are exposed on the surface, which in turn can cause chain-chain hydrophobic interaction where surfactants can get adsorbed to the surface with their tails. At the same time, their polar heads make the surface more hydrophilic (Somasundaran and Zhang, 2006).

For AOT, SDBS, and their brine combinations, the viscosity ratios are very similar, and so is the level of displacement stability. Viscous fingering is observed in all the tests. The patterns are also similar with about the same degree of branching. Contrary to the brine floods, surfactants do not go through a very unstable oil recovery after the breakthrough. Instead, they steadily recover additional oil droplets in form of oil-in-water emulsions at a slow pace. All of these tests were stopped after reaching 4.8 PV s.

According to Fig. 6, independent of the rock wettability, AOT responded positively to mixing with both low and high salinity brine in terms of oil recovery. SDBS, when mixed with high salinity water, also recovers more oil, while it decreases the recovery when used with low salinity brine. There can be optimum salinities for different surfactants. Therefore, it can be deduced that mixing brine with surfactant solution can be beneficial if used at optimum ionic strength. Studies in the past have also reported increased recovery from brine-surfactant flooding (Alagic and Skauge, 2010; Glover et al., 1979; Johannessen and Spildo, 2013; Spildo et al., 2014). Nourani et al. (2014), showed lower surfactant adsorption on hydrophilic surfaces for both SDBS and AOT when the surfactants are combined with low salinity brine through quartz crystal microbalance (QCM) measurements. In addition, they showed that oil desorption is higher for LS-surfactant than surfactant-only from silica surfaces. Salt can also have a negative effect depending on the concentration. At low salt concentration, the surfactant has good solubility in the water phase. At the optimum salinity, surfactant dissolves in both phases and leads to a minimum IFT (El-Batanoney et al., 1999). The measured CMC's by Tichelkamp et al. (2014) were 1.69 mmol/L for SDBS and 2.55 mmol/L for AOT both in DI water. At higher salt concentrations, CMC decreases.

Generally comparing the two types of surfactant, in hydrophobic networks, AOT solutions recovered on average 1.0%–15.5% higher. However, in hydrophilic networks, AOT has a higher recovery dissolved in low salinity brine, whereas SDBS has a higher recovery dissolved in high salinity brine. The capillary numbers for the SDBS and AOT solutions in DI water as the flood are 1.4E-5 and 2.9E-5, respectively. Although the capillary number for one is more than two times the other, the difference in recovery factor is only 1.8% in favor of SDBS in the water-wet model and 5.3% higher for AOT in the oil-wet model. The contact angle measurements from the micrographs in hydrophilic tests revealed 19 ± 9° and 10 ± 3° for HS-AOT and HS-SDBS, respectively. This can contribute to the explanation for higher recovery of oil by HS-SDBS. In hydrophobic tests, the angles are 162 ± 6° and almost 180 for HS-SDBS and HS-AOT, respectively. Hematpour et al. (2012b) reported higher RF for the linear surfactant in glass chips, which is consistent with our result for the surfactant in DI water and high salinity surfactant tests. Nourani et al. (2014) reported that SDBS showed lower adsorption than AOT on both silica and aluminosilicate surfaces in QCM measurements. Besides, they measured higher oil desorption for LS-AOT than LS-SDBS from both hydrophilic and hydrophobic surfaces.

One fundamental difference between brine and surfactant floods in this study is that in the latter, the oil saturation keeps decreasing as long as the surfactant flood is being injected. The brine flood recovery

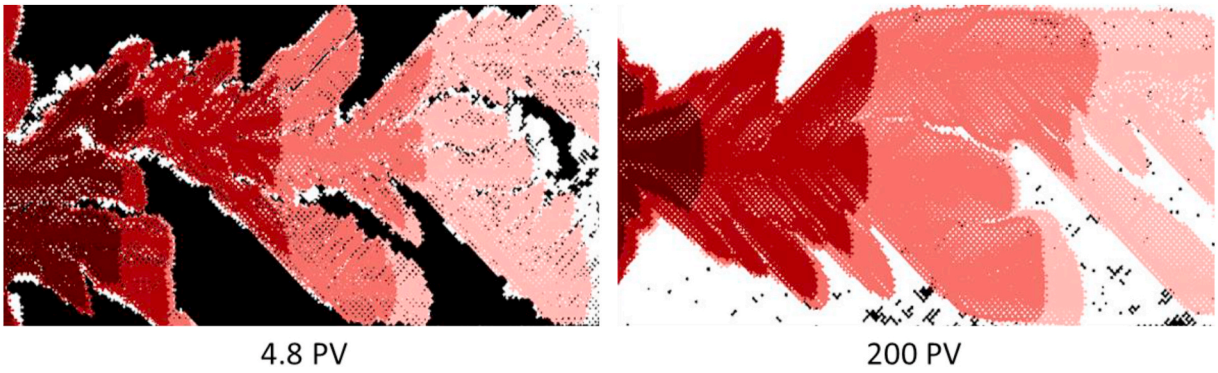

Fig. 7. The progress of crude oil A being displaced by HS-AOT in two uniform hydrophilic networks using different amounts of the flood. The early stage is represented by the darkest color, and the breakthrough by the lightest pink. The white area shows the amount of oil recovered after the breakthrough. The voids of the chip (grains) are colored with the same color as the surrounding channels. (For interpretation of the references to color in this figure legend, the reader is referred to the Web version of this article.)

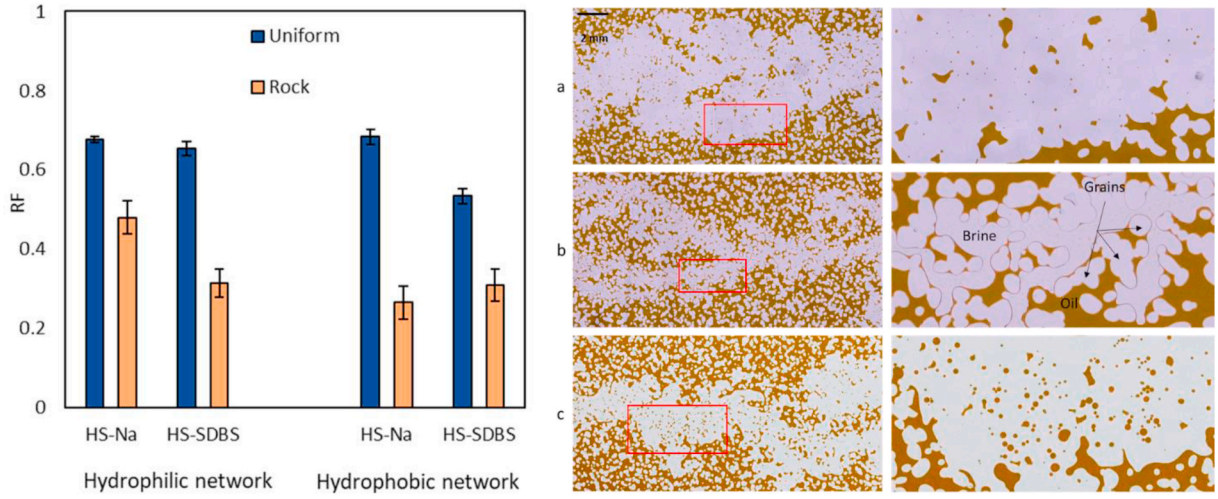

Fig. 8. On the left: RF for crude oil A displaced by high salinity brine and surfactant floods in different micromodel designs with different wettabilities. On the right: After-flood images of crude oil A displaced by (a) HS-Na in a water-wet chip, (b) HS-Na in an oil-wet chip, and (c) HS-SDBS in a water-wet chip.

reaches a plateau, usually shortly after the breakthrough. However, the much lower interfacial tension with surfactants causes the continued recovery after the breakthrough. One long running test showed a 97% recovery of crude oil A in a hydrophilic network after injecting about 200 pore volumes of the HS-AOT. However, a similar test for a brine flood showed no additional recovery. Therefore, depending on the flood volume at any point, the surfactant recovery can be higher or lower than brine recovery.

Fig. 7 shows the progress of high salinity AOT through the oil-saturated chip. The light pink color represents the breakthrough. The white area shows the extra oil that is recovered after the breakthrough until the entire volume of the flood is injected. Figure S3 better demonstrates the difference between brine and surfactant flooding in a dynamic recovery graph. Once the low salinity brine reaches breakthrough, the recovery reaches a plateau, whereas the LS-SDBS flood continues extracting oil from the channels through emulsification. The horizontal lines through the last data points better show the improvement in recovery since the breakthrough. The continued recovery mainly happens in the form of oil droplets getting released from the pores and throats or oil-water interface and suspending in the water phase towards the outlet. The movement of the interface between the bulk of the oil and flood also contributes to the overall recovery. In the water-wet network, the profile of the flood pattern grows in the same shape as it was at breakthrough, whereas in the oil-wet network the outline changes by moving the bulk of the oil in places closest to the main flood stream. If the surfactant flow continues long enough, all the oil gets recovered. This process, however, is much slower for hydrophobic networks. Surfactant flood also reaches breakthrough in a shorter amount of time. However favorable, the use of surfactant in large volumes would not be economically justified as a secondary recovery method. Therefore, this makes a suitable option for the tertiary recovery, where seawater flooding is employed as the secondary stage; once it cannot recover additional oil, surfactant flooding can increase the production. This will be presented in Section 3.2.4.

3.2.3. Network design

All presented results so far have been carried out in uniform networks as the ideal design for fundamental studies. However, the impact of the network design on oil recovery is also important. Therefore, some experiments were conducted to evaluate the recovery in the more realistic rock design micromodels (of both oil-wet and water-wet conditions) with brine and high salinity surfactant flooding. The results are presented in Fig. 8 (left).

Based on the graph, regardless of the surface wettability or flood

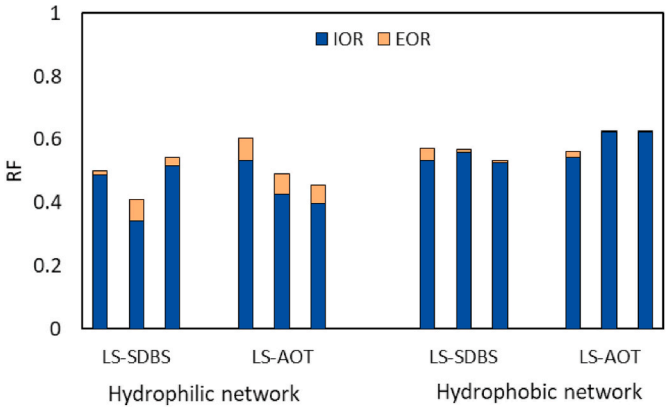

Fig. 9. Recovery of crude oil A by IOR and EOR flood, with HS-Na as IOR flood, and LS-SDBS and LS-AOT as EOR floods in uniform networks. Each bar represents a single measurement.

type, all rock network tests resulted in a significantly lower oil recovery than uniform network tests. This outcome is explained by the inherent characteristics of the rock with dead-end or smaller pores. Fig. 8 also shows the oil-brine arrangement in the water-wet and oil-wet channels of the rock networks. The pore-scale observation reveals the layers of oil covering the hydrophobic network, especially on the angled parts between grains (Fig. 8b). It is also a similar situation with HS-SDBS, but with less amount of oil bound to the surface. These structures and trapped oil layers do not exist in the uniform network, which contributes to the higher RF in uniform networks. Fig. 8a shows some residual trapped oil left in the flood path, and Fig. 8c shows some mobilized oil droplets by the surfactant. Furthermore, Figure S4 shows the progress of the HS-SDBS through the hydrophilic rock network, and the amount of additional oil recovered after the breakthrough.

3.2.4. Low salinity surfactant EOR

Utilizing both surfactant and brine floods was suggested to have functional, environmental and economic justification for chemical EOR (Alagic and Skauge, 2010; Glover et al., 1979; Johannessen and Spildo, 2013; Spildo et al., 2014). The EOR tests were designed based on the procedure from an earlier study to simulate the oil recovery process from the reservoir rock.

The EOR experiments, as described in the experimental procedure section, are conducted using low salinity surfactant solutions as the EOR

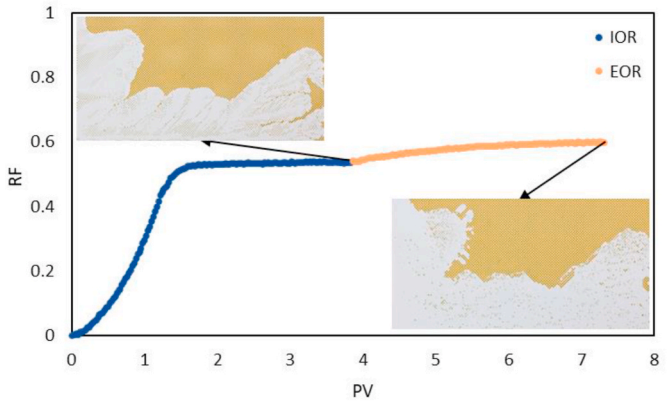

Fig. 10. Dynamic recovery of crude oil A based on pore volumes of HS-Na (IOR) followed by LS-AOT (EOR) in a hydrophilic network.

flood. The results for the tests in both hydrophilic and hydrophobic micromodels are presented in Fig. 9.

According to Fig. 9, AOT is more effective at the tertiary recovery stage in water-wet chips (6.6% vs 3.5%), while SDBS proved to be slightly more effective for oil-wet chips (1.8% vs 0.8%). Based on Fig. 6, LS-AOT in a one-step recovery in hydrophilic networks was also more effective than LS-SDBS. Khanamiri et al. (2016), carried out sandstone core flooding tests with low salinity SDBS solutions. They reported a 2.4–6.2% EOR recovery factor, depending on different calcium to sodium ratios. Alagic et al. (Alagic and Skauge, 2010; Alagic et al., 2011) reported an overall recovery of approximately 40–80% for low salinity surfactant based on different aging times and surfactant concentrations. Although our results are consistent with the literature in recovering additional oil by using surfactant floods, making direct number comparisons would be valid only if all procedures and parameters were the same.

Fig. 10 demonstrates both stages of crude oil A recovery by LS-AOT following HS-Na in a hydrophilic micromodel. The brine solution breaks through the network by pushing the oil in bulk until about1.5 pore volume, reaching 53.2% IOR recovery factor by the time EOR flood reaches the network. Subsequently, surfactant starts producing oil again by mobilizing the oil trapped in the channels or detaching oil globules from the oil-water interface. A small part of extra recovery can also be caused by the movement of the interface towards the outlet due to pressure difference. In this way, another 7.4% of the original oil in place was extracted in the tertiary recovery. The two pictures on the graph also mark the state of the network at the end of IOR and EOR flooding. The recovery process is similar for the LS-SDBS tests as well. The patterns for the hydrophobic models are very similar to that in Fig. 3. The process of EOR recovery is controlled by the movement of bigger globules of oil due to the flow and pressure difference and to a smaller extent by the suspended oil droplets.

Fig. 11 shows how the two phases arrange and change contact angle through different recovery stages for LS-AOT EOR test. The images for the LS-SDBS EOR tests also look similar to those in the figure. The change caused by the EOR flood in the hydrophilic network is more substantial than the hydrophobic one, as is the amount of recovery. The EOR flood creates small mobilized oil globules that do not coalesce with each other or get stuck in the channels due to surfactant adsorption at the interface. The change in the hydrophobic network caused by the EOR flood is more subtle. The figure also shows thin layers of oil adsorbed on the oil-wet surface. Hydrophobic chips trap more irreducible water than hydrophilic ones from the initial brine saturation step. It also takes longer for the flood to reach the network in oil-wet chips. Although the IOR flood recovers more oil from the hydrophobic network, the extra amount of oil extracted by the EOR floods are generally lower than EOR recoveries in hydrophilic chips.

4. Conclusions

Rock wettability plays a vital role in the mobilization and displacement of crude oil in pore models. In this study, a silanization process was

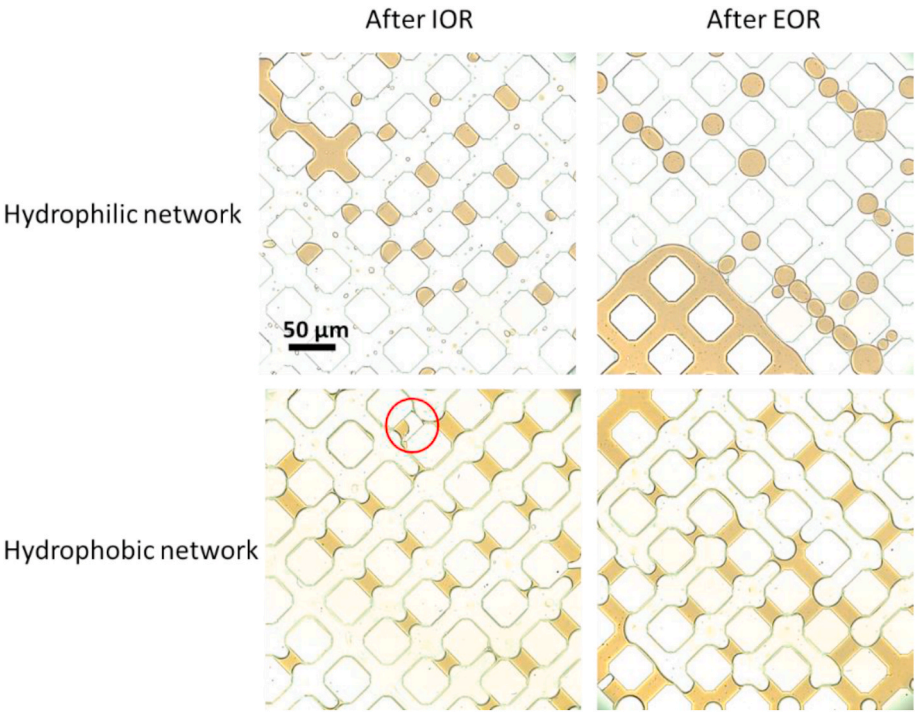

Fig. 11. Micrographs of remaining oil (crude oil A) after the IOR (HS–Na) and EOR (LS-AOT) flood in water- and oil-wet networks. The red mark shows the irreducible water representing connate water. (For interpretation of the references to color in this figure legend, the reader is referred to the Web version of this article.)

used to alter the wettability of the micromodels. Utilizing our previously developed methodology, experiments were conducted while varying oil- and water-phase parameters, and network properties. Some parameters, including salt concentration and presence of divalent ions, showed opposite effects on the recovery based on the surface wettability. The less viscous crude oil had a more efficient recovery from both water- and oil-wet chips. Independent of test conditions, the rock network showed lower recovery than the uniform one. Moreover, surfactants showed some promising results in recovering additional oil beyond breakthrough, even if they are used as the tertiary stage after the brine has reached a plateau. This positive effect was especially profound for the hydrophilic networks. Depending on the ionic strength and surface wettability, combining surfactant with brine can positively or negatively affect the amount of oil recovered at breakthrough. In EOR tests, between the two surfactants, LS-AOT worked more efficiently in the hydrophilic network, while LS-SDBS performed better in the oil-wet systems. There still is great potential for more tests on this subject utilizing microfluidics as the newer and less-explored option for oil recovery studies. Additional tests at conditions closer to actual reservoir conditions can be of significance. Microfluidic tests along with validation tests using core flooding can also be beneficial to the fundamental understanding of the processes.

Author contribution

Marzieh Saadat: method development, experimental work, data Formal analysis, and manuscript preparation. Junyi Yang: experimental work, and manuscript review. Marcin Dudek: Supervision of the work, discussion of the results, and manuscript review. Gisle Øye: Supervision of the work, discussion of the results, and manuscript review. Peichun A. Tsai: Supervision of the work done at University of Alberta, Canada, discussion of the results, and manuscript review.

Declaration of competing interest

The authors declare that they have no known competing financial interests or personal relationships that could have appeared to influence the work reported in this paper.

Acknowledgement

This project was funded by VISTA, a research partnership between Equinor and the Norwegian Academy of Science and Letters (project number 6365). Moreover, we would like to thank Roar Skartlien and Meysam Nourani for their comments and discussions. The project was also supported by the Canada First Research Excellence Fund (CFREF), the Future Energy System (FES) at the University of Alberta *via* Project T02-P05, and the Canada Foundation for Innovation (NSERC CFI) Grant 34546. P. A. T. holds a Canada Research Chair in Fluids and Interfaces and gratefully acknowledges funding from the Natural Sciences and Engineering Research Council of Canada (NSERC) and Alberta Innovates (AI).

References

Alagic, E., Skauge, A., 2010. Combined low salinity brine injection and surfactant flooding in mixed-wet sandstone cores (vol 24, pg 3551, 2010). Energy Fuel. 24 (12), 6696, 6696.
Alagic, E., Spildo, K., Skauge, A., Solbakken, J., 2011. Effect of crude oil ageing on low salinity and low salinity surfactant flooding. J. Petrol. Sci. Eng. 78 (2), 220–227.
Alshakhs, M.J., Kovscek, A.R., 2016. Understanding the role of brine ionic composition on oil recovery by assessment of wettability from colloidal forces. Adv Colloid Interfac 233, 126–138.
Alvarado, V., Garcia-Olvera, G., Hoyer, P., Lehmann, T.E., 2014. Impact of Polar Components on Crude Oil-Water Interfacial Film Formation: A Mechanisms for Low-Salinity Waterflooding, SPE Annual Technical Conference and Exhibition. Society of Petroleum Engineers, Amsterdam, The Netherlands, p. 15.
Anderson, W.G., 1987. Wettability literature survey Part 5: the effects of wettability on relative permeability. SPE-129421-JPT 39 (11), 1453–1468.
Arkles, B., 1977. Tailoring surfaces with silanes. Chemtech 7, 766–778.
Austad, T., Rezaeidoust, A., Puntervold, T., 2010. Chemical mechanism of low salinity water flooding in sandstone reservoirs. In: SPE Improved Oil Recovery Symposium. Society of Petroleum Engineers, Tulsa, Oklahoma, USA, p. 17.
Austad, T., Standnes, D.C., 2003. Spontaneous imbibition of water into oil-wet carbonates. J. Petrol. Sci. Eng. 39 (3–4), 363–376.
Bera, A., Mandal, A., 2015. Microemulsions: a novel approach to enhanced oil recovery: a review. J Pet Explor Prod Te 5 (3), 255–268.
Bobek, J.E., Mattax, C.C., Denekas, M.O., 1958. Reservoir rock wettability - its significance and evaluation. SPE-895-G 213 (1), 155–160.
Buchgraber, M., Al-Dossary, M., Ross, C.M., Kovscek, A.R., 2012. Creation of a dual-porosity micromodel for pore-level visualization of multiphase flow. J. Petrol. Sci. Eng. 86–87, 27–38.
Buckley, J.S., Liu, Y., 1998. Some mechanisms of crude oil/brine/solid interactions. J. Petrol. Sci. Eng. 20, 155–160.
Chavez-Miyauchi, T.E., Firoozabadi, A., Fuller, G.G., 2016. Nonmonotonic elasticity of the crude oil-brine interface in relation to improved oil recovery. Langmuir 32 (9), 2192–2198.
Ding, H., Rahman, S., 2017. Experimental and theoretical study of wettability alteration during low salinity water flooding-an state of the art review. Colloid. Surface. Physicochem. Eng. Aspect. 520, 622–639.
Dubey, N., 2009. Thermodynamic properties of micellization of sodium dodecylbenzene sulfonate in the aqueous-rich region of 1-pentanol and 1-hexanol. J. Chem. Eng. Data 54 (3), 1015–1021.
Dudek, M., Bertheussen, A., Dumaire, T., Øye, G., 2018. Microfluidic tools for studying coalescence of crude oil droplets in produced water. Chem. Eng. Sci. 191, 448–458.
Eckstein, Y., 1988. Role of silanes in adhesion-Part I. Dynamic mechanical properties of silane coatings on glass fibers. J. Adhes. Sci. Technol. 2 (1), 339–348.
El-Batanoney, M., Abdel-Moghny, T., Ramzi, M., 1999. The effect of mixed surfactants on enhancing oil recovery. J. Surfactants Deterg. 2 (2), 201–205.
Farooq, U., Asif, N., Tweheyo, M.T., Sjoblom, J., Oye, G., 2011. Effect of low-saline aqueous solutions and pH on the desorption of crude oil fractions from silica surfaces. Energy Fuel. 25 (5), 2058–2064.
Fathi, S.J., Austad, T., Strand, S., 2011. Effect of water-extractable carboxylic acids in crude oil on wettability in carbonates. Energy Fuel. 25 (6), 2587–2592.
Flynn, P.F., Wand, A.J., 2001. High-resolution nuclear magnetic resonance of encapsulated proteins dissolved in low viscosity fluids. Methods Enzymol. 339, 54–70.
Forland, G.M., et al., 1998. Influence of alcohol on the behavior of sodium dodecylsulfate micelles. J. Colloid Interface Sci. 203 (2), 328–334.
Glover, C.J., Puerto, M.C., Maerker, J.M., Sandvik, E.L., 1979. Surfactant phase behavior and retention in porous media. SPE-7053-PA 19 (3), 183–193.
Grate, J.W., et al., 2013. Silane modification of glass and silica surfaces to obtain equally oil-wet surfaces in glass-covered silicon micromodel applications. Water Resour. Res. 49 (8), 4724–4729.
Hait, S.K., Majhi, P.R., Blume, A., Moulik, S.P., 2003. A critical assessment of micellization of sodium dodecyl benzene sulfonate (SDBS) and its interaction with poly(vinyl pyrrolidone) and hydrophobically modified polymers, JR 400 and LM 200. J. Phys. Chem. B 107 (15), 3650–3658.
Hajibagheri, F., Lashkarbolooki, M., Ayatollahi, S., Hashemi, A., 2017. The synergic effects of anionic and cationic chemical surfactants, and bacterial solution on wettability alteration of carbonate rock: an experimental investigation. Colloid. Surface. 513, 422–429.
He, K., et al., 2014. Validating surfactant performance in the eagle ford shale: a correlation between the reservoir-on-a-chip approach and enhanced well productivity. In: SPE Improved Oil Recovery Symposium. Society of Petroleum Engineers.
He, K., Xu, L., Gao, Y., Yin, X., Neeves, K.B., 2015. Evaluation of surfactant performance in fracturing fluids for enhanced well productivity in unconventional reservoirs using Rock-on-a-Chip approach. J. Petrol. Sci. Eng. 135, 531–541.
Hematpour, H., Arabjamloei, R., Nematzadeh, M., Esmaili, H., Mardi, M., 2012a. An experimental investigation of surfactant flooding efficiency in low viscosity oil using a glass micromodel. Energy Sources, Part A Recovery, Util. Environ. Eff. 34 (19), 1745–1758.
Hematpour, H., Arabjamloei, R., Nematzadeh, M., Esmaili, H., Mardi, M., 2012b. An experimental investigation of surfactant flooding efficiency in low viscosity oil using a glass micromodel. Energy Sources Part A 34 (19), 1745–1758.
Howe, A.M., et al., 2015. Visualising surfactant enhanced oil recovery. Colloid. Surface. Physicochem. Eng. Aspect. 480, 449–461.
Jakobsen, T.D., Simon, S., Heggset, E.B., Syverud, K., Paso, K., 2018. Interactions between surfactants and cellulose nanofibrils for enhanced oil recovery. Ind. Eng. Chem. Res. 57 (46), 15749–15758.
Jamaloei, B.Y., Kharrat, R., 2010. Analysis of microscopic displacement mechanisms of dilute surfactant flooding in oil-wet and water-wet porous media. Transport Porous Media 81 (1), 1.
Jing, D.L., Bhushan, B., 2013. Quantification of surface charge density and its effect on boundary slip. Langmuir 29 (23), 6953–6963.
Johannessen, A.M., Spildo, K., 2013. Enhanced oil recovery (EOR) by combining surfactant with low salinity injection. Energy Fuel. 27 (10), 5738–5749.
Ju, B., Fan, T., Ma, M., 2006. Enhanced oil recovery by flooding with hydrophilic nanoparticles. China Particuol. 4 (1), 41–46.
Kamal, M.S., Hussein, I.A., Sultan, A.S., 2017. Review on surfactant flooding: phase behavior, retention, IFT, and field applications. Energy Fuel. 31 (8), 7701–7720.
Katende, A., Sagala, F., 2019. A critical review of low salinity water flooding: mechanism, laboratory and field application. J. Mol. Liq. 278, 627–649.

Kelesoglu, S., Volden, S., Kes, M., Sjoblom, J., 2012. Adsorption of naphthenic acids onto mineral surfaces studied by quartz crystal microbalance with dissipation monitoring (QCM-D). Energy Fuel. 26 (8), 5060–5068.
Khanamiri, H.H., et al., 2016. EOR by low salinity water and surfactant at low concentration: impact of injection and in situ brine composition. Energy Fuel. 30 (4), 2705–2713.
Kowalewski, E., Holt, T., Torsaeter, O., 2002. Wettability alterations due to an oil soluble additive. J. Petrol. Sci. Eng. 33 (1–3), 19–28.
Lager, A., Webb, K.J., Black, C.J.J., Singleton, M., Sorbie, K.S., 2008a. Low salinity oil recovery - an experimental investigation. Petrophysics 49 (1), 28–35.
Lager, A., Webb, K.J., Collins, I.R., Richmond, D.M., 2008b. LoSal Enhanced Oil Recovery: Evidence of Enhanced Oil Recovery at the Reservoir Scale, SPE Symposium on Improved Oil Recovery. Society of Petroleum Engineers, Tulsa, Oklahoma, USA, p. 12.
Lifton, V.A., 2016. Microfluidics: an enabling screening technology for enhanced oil recovery (EOR). Lab Chip 16 (10), 1777–1796.
Ligthelm, D.J., et al., 2009. Novel Waterflooding Strategy by Manipulation of Injection Brine Composition, EUROPEC/EAGE Conference and Exhibition. Society of Petroleum Engineers, Amsterdam, The Netherlands, p. 22.
Lutzenkirchen, J., Richter, C., 2013. Zeta-potential measurements of OTS-covered silica samples. Adsorption 19 (2–4), 217–224.
Mahani, H., Berg, S., Ilic, D., Bartels, W.-B., Joekar-Niasar, V., 2013. Kinetics of the low salinity waterflooding effect studied in a model system. In: SPE Enhanced Oil Recovery Conference. Society of Petroleum Engineers, Kuala Lumpur, Malaysia, p. 14.
McGuire, P.L., Chatham, J.R., Paskvan, F.K., Sommer, D.M., Carini, F.H., 2005. Low Salinity Oil Recovery: an Exciting New EOR Opportunity for Alaska's North Slope, SPE Western Regional Meeting. Society of Petroleum Engineers, Irvine, California, p. 15.
Mohammed, M., Babadagli, T., 2015. Wettability alteration: a comprehensive review of materials/methods and testing the selected ones on heavy-oil containing oil-wet systems. Adv Colloid Interfac 220, 54–77.
Morrow, N., Buckley, J., 2011. Improved oil recovery by low-salinity waterflooding. SPE-129421-JPT 63 (5), 106–112.
Morrow, N.R., 1990. Wettability and its effect on oil recovery. SPE-129421-JPT 42 (12), 1476–1484.
Naik, V.V., Crobu, M., Venkataraman, N.V., Spencer, N.D., 2013. Multiple transmission-reflection IR spectroscopy shows that surface hydroxyls play only a minor role in alkylsilane monolayer formation on silica. J. Phys. Chem. Lett. 4 (16), 2745–2751.
Nilsson, M.A., et al., 2013. Effect of fluid rheology on enhanced oil recovery in a microfluidic sandstone device. J. Non-Newtonian Fluid Mech. 202, 112–119.
Nourani, M., Tichelkamp, T., Gawel, B., Oye, G., 2014. Method for determining the amount of crude oil desorbed from silica and aluminosilica surfaces upon exposure to combined low-salinity water and surfactant solutions. Energy Fuel. 28 (3), 1884–1889.
Nourani, M., Tichelkamp, T., Gaweł, B., Øye, G., 2016. Desorption of crude oil components from silica and aluminosilicate surfaces upon exposure to aqueous low salinity and surfactant solutions. Fuel 180, 1–8.
Ogunberu, A.L., Ayub, M., 2005. The role of wettability in petroleum recovery. Petrol. Sci. Technol. 23 (2), 169–188.
Pradilla, D., et al., 2016. Microcalorimetry study of the adsorption of asphaltenes and asphaltene model compounds at the liquid-solid surface. Langmuir 32 (29), 7294–7305.
RezaeiDoust, A., Puntervold, T., Austad, T., 2011. Chemical verification of the EOR mechanism by using low saline/smart water in sandstone. Energy Fuel. 25 (5), 2151–2162.
Saadat, M., Tsai, P.A., Ho, T.-H., Øye, G., Dudek, M., 2020. Development of a microfluidic method to study enhanced oil recovery by low salinity water flooding. ACS Omega 5 (28), 17521–17530.
Schneider, M.H., Tabeling, P., 2011. Lab-on-Chip methodology in the Energy industry: wettability patterns and their impact on fluid displacement in oil reservoir models. Am. J. Appl. Sci. 8, 927–932.
Seccombe, J.C., Lager, A., Webb, K.J., Jerauld, G., Fueg, E., 2008. Improving wateflood recovery: LoSalTM EOR field evaluation. In: SPE Symposium on Improved Oil Recovery. Society of Petroleum Engineers, Tulsa, Oklahoma, USA, p. 19.
Sharma, H., Mohanty, K.K., 2018. An experimental and modeling study to investigate brine-rock interactions during low salinity water flooding in carbonates. J. Petrol. Sci. Eng. 165, 1021–1039.
Sheng, J.J., 2014. Critical review of low-salinity waterflooding. J. Petrol. Sci. Eng. 120, 216–224.
Somasundaran, P., Zhang, L., 2006. Adsorption of surfactants on minerals for wettability control in improved oil recovery processes. J. Petrol. Sci. Eng. 52 (1–4), 198–212.
Song, W., Kovscek, A.R., 2015. Functionalization of micromodels with kaolinite for investigation of low salinity oil-recovery processes. Lab Chip 15 (16), 3314–3325.
Song, W., Kovscek, A.R., 2016. Direct visualization of pore-scale fines migration and formation damage during low-salinity waterflooding. J. Nat. Gas Sci. Eng. 34, 1276–1283.
Spildo, K., Johannessen, A.M., Skauge, A., 2012. Low salinity waterflood at reduced capillarity. In: SPE Improved Oil Recovery Symposium.
Spildo, K., Sun, L.M., Djurhuus, K., Skauge, A., 2014. A strategy for low cost, effective surfactant injection. J. Petrol. Sci. Eng. 117, 8–14.
Stein, D., Kruithof, M., Dekker, C., 2004. Surface-charge-governed ion transport in nanofluidic channels. Phys. Rev. Lett. 93 (3).
Subramanian, S., Buscetti, L., Simon, S., Sacre, M., Sjoblom, J., 2018. Influence of fatty-alkylamine amphiphile on the asphaltene adsorption/deposition at the solid/liquid interface under precipitating conditions. Energy Fuel. 32 (4), 4772–4782.
Tang, G.Q., Morrow, N.R., 1997. Salinity, temperature, oil composition, and oil recovery by waterflooding. SPE Reservoir Eng. 12 (4), 269–276.
Tichelkamp, T., et al., 2016. EOR potential of mixed alkylbenzenesulfonate surfactant at low salinity and the effect of calcium on "optimal ionic strength". Energy Fuel. 30 (4), 2919–2924.
Tichelkamp, T., Teigen, E., Nourani, M., Øye, G., 2015. Systematic study of the effect of electrolyte composition on interfacial tensions between surfactant solutions and crude oils. Chem. Eng. Sci. 132, 244–249.
Tichelkamp, T., Vu, Y., Nourani, M., Øye, G., 2014. Interfacial tension between low salinity solutions of sulfonate surfactants and crude and model oils. Energy Fuel. 28 (4), 2408–2414.
Wagner, O.R., Leach, R.O., 1959. Improving oil displacement efficiency by wettability adjustment. SPE-895-G 216 (1), 65–72.
Wang, L.Z., Mohanty, K., 2015. Enhanced oil recovery in gasflooded carbonate reservoirs by wettability-altering surfactants. SPE J. 20 (1), 60–69.
Wegner, J., Hincapie, R.E., Födisch, H., Ganzer, L., 2015. Novel visualisation of chemical EOR flooding using a lab-on-a-chip setup supported by an extensive rheological characterisation. In: SPE Asia Pacific Enhanced Oil Recovery Conference. Society of Petroleum Engineers, Kuala Lumpur, Malaysia, p. 15.
Yousef, A.A., Al-Saleh, S., Al-Jawfi, M.S., 2012. Improved/enhanced oil recovery from carbonate reservoirs by tuning injection water salinity and ionic content. In: SPE Improved Oil Recovery Symposium. Society of Petroleum Engineers, Tulsa, Oklahoma, USA, p. 18.
Yu, M., et al., 2019. Effects of fines migration on oil displacement by low-salinity water. J. Petrol. Sci. Eng. 175, 665–680.
Zhang, C.Y., Oostrom, M., Wietsma, T.W., Grate, J.W., Warner, M.G., 2011. Influence of viscous and capillary forces on immiscible fluid displacement: pore-scale experimental study in a water-wet micromodel demonstrating viscous and capillary fingering. Energy Fuel. 25 (8), 3493–3505.
Zhang, P., Austad, T., 2005. The relative effects of acid number and temperature on chalk wettability. In: SPE International Symposium on Oilfield Chemistry. Society of Petroleum Engineers, The Woodlands, Texas, p. 7.